
**ANALYTICAL STUDY OF INTERFACE BEHAVIOR OF ONE-WAY
COMPOSITE PRE-SLABS WITH H.S.C TOP LAYER UNDER
DIFFERENT CASES OF LOADING AND PERCENTAGE OF SHEAR
CONNECTORS**

M.M El-Hawary⁽¹⁾, M. Rabie⁽²⁾ and W.Zaki⁽³⁾

⁽¹⁾Teaching Assistant, Construction Engineering Department, Misr University for
Science &Technology

⁽²⁾ Professor of Reinforced Concrete Structures, Structural Engineering Department, Faculty of
Engineering, Cairo University

⁽³⁾ Assistant Professor of Reinforced Concrete Structures, Structural Engineering Department,
Faculty of Engineering, Beni-Suef University

Abstract

This paper presents a numerical analysis using ANSYS (18.1) finite element program to simulate the reinforced concrete slabs; six monolithic slabs and eight composite pre-slabs; Both the monolithic and pre-slabs had been supported on two edge supports to represent the case of one way simply supported slab. Fourteen slabs with length 1060mm, width 800mm, and thickness 100mm were modelled. The finite element model describes the used reinforced concrete element, the modelling of concrete, the modelling of reinforcement bars, modelling of shear connector bars and the modelling of interface element connecting the two concretes (high strength & normal strength). The results showed that the general behavior of the finite element models represented by the ultimate load, shear transfer, load-deflection curves. Show good agreement with the test results from the experimental program.

Keywords: Finite element- Shear connectors- Deflection

Introduction

Ms. R. Sangeetha, et al [1] stated that Composite construction exists when two different materials are bound together so strongly that they act together as a single unit from a structural point of view. When this occurs, it is called composite action. It is the dominant form of construction for the multi-story building sector. This has been the case for over twenty years. Its success is due to the strength and stiffness that can be achieved, with minimum use of materials. The reason why composite construction is often so good can be expressed in one simple way - concrete is good in compression and steel is good in tension. By joining the two materials together structurally these strengths can be exploited to result in a highly efficient design. The

reduced self-weight of composite elements has a knock-on effect by reducing the forces in those elements supporting them, including the foundations.

Composite systems also offer speed of construction benefits, which were a key reason for the boom in use of steel for commercial buildings in the UK in the 1980s. The floor depth reductions that can be achieved using composite construction can also provide significant benefits in terms of the costs of services and the building envelope.

Kovach, J., & Naito, C., [2] Previous research and observations of the horizontal shear capacity of composite concrete sections have been conducted since the 1950s. There were several experimental programs performed to determine the horizontal shear stress of a composite section's interface.

M. Rabie, [3] Composite sections are the use of two or many dissimilar or similar materials in one section, which are working together as a one unit. Concrete-concrete composite flexural members are widely used in buildings and bridges construction as well as strengthening. Most of the recent codes of practice permit design of composite flexural member as monolithic one provided that its composite interface has enough shear transfer capacity. The increase of composite interface roughness and the use of steel ties, shear keys or adhesive materials, improve the shear transfer capacity and thus insure the full composite action.

Abd El-Hay A.S [4] stated that the common types of the composite concrete-concrete sections are composite slabs with either deck floor or prefabricated beam. The transfer of shear across the interface plane between the old and new concrete layers is called “shear transfer” to distinguish this type of shearing action from that which usually occurs in reinforced concrete beams.

Details of the tested specimens

Monolithic Slab Specimens

Experimental program was carried out on six monolithic slabs; The slab was supported on two edge supports to represent the case of one way simply supported slab. Each monolithic slab consists of one concrete layer with dimensions 1060*800*100mm with main bottom reinforcement of 10Φ12 mm and secondary reinforcement of 6Φ6 mm as shown in **Figure1, 2**.

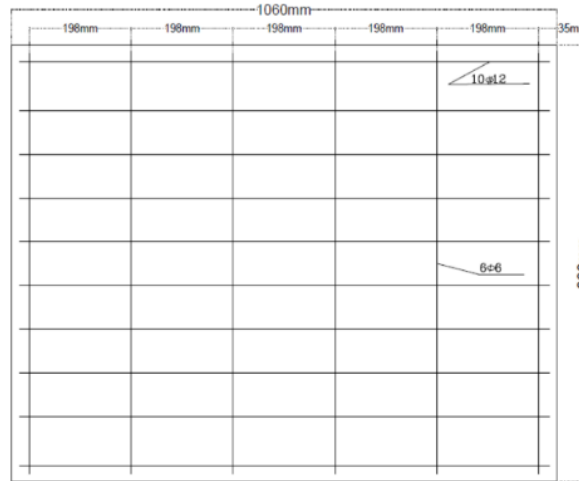


Fig 1: General specimen's details

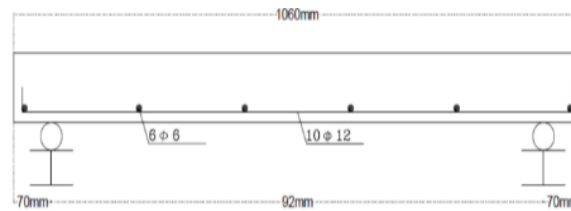


Fig 2: Monolithic specimen's details

Composite Pre-Slab Specimens

Experimental program was carried out on eight composite pre-slabs; all slabs were supported on two edge supports to represent the case of one way simply supported slabs. Each composite slab consists of two concrete layers; the first layer was slab with dimensions 1060*800*50 mm with main bottom reinforcement of 10Φ12 mm, secondary reinforcement of 6Φ6 mm and its $f_{cu}=35$ N/mm². The second layer had the same dimensions as the first layer 1060*800*50 mm without reinforcement and its $f_{cu}=60$ N/mm² as shown in the **figure 3**.

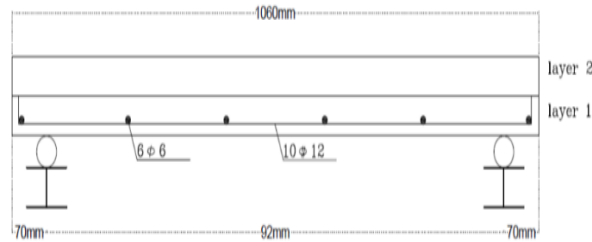


Fig 3: Pre-slab specimen's details

Finite element modelling by “ANSYS” program

The finite element model describes the used reinforced concrete element, the modelling of concrete, the modelling of reinforcement bars, modelling of shear connector bars and the modelling of interface element connecting the two concrete (high strength & normal strength) concrete layers.

Element type
Concrete element

The solid65 is used 3-d modelling of concrete with or without reinforcing steel; Also, solid65 element is capable of cracking in tension and crushing in compression. The multi linear isotropic concrete model uses the von Mises failure to define the failure of concrete.

The solid65 element models the nonlinear response of reinforced concrete. The behavior of the concrete material is based on a constitutive model for the triaxial behavior of concrete. Solid 65 is capable of plastic deformation, cracking in three orthogonal directions at each integration point. The cracking is modelled through an adjustment of the material properties that is done by changing the element stiffness matrices. If the concrete at an integration point fails in uniaxial, biaxial, or triaxial compression, the concrete is assumed crushed at that point. Crushing is defined as the complete deterioration of the structural integrity of the concrete. A schematic of the element is shown in **Figure 4 and 5**.

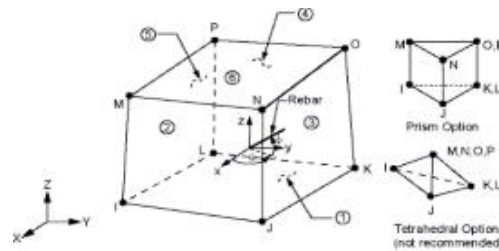


Figure 4: Solid65 Element (ANSYS 18.1)

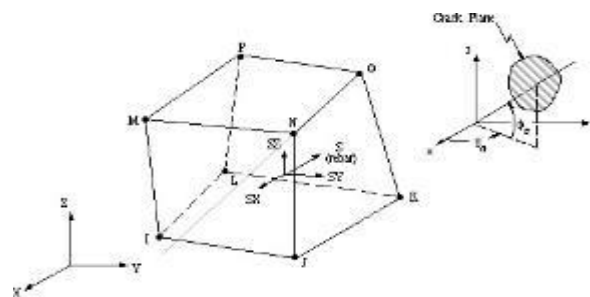


Figure 5: Solid65 Element stress output (ANSYS 18.1)

Shear Connectors

BEAM4 is used for modelling of steel shear connectors, which defined by two or three nodes. BEAM4 is a uniaxial element with tension, compression, torsion, and bending capabilities. The

element has six degrees of freedom at each node: translations in the nodal x, y, and z directions and rotations about the nodal x, y, and z axes. Stress stiffening and large deflection capabilities are included. A consistent tangent stiffness matrix option is available for use in large deflection (finite rotation) analyses. The geometry, node locations, and coordinate systems for this element and stress output are shown in **figures 6 and 7**.

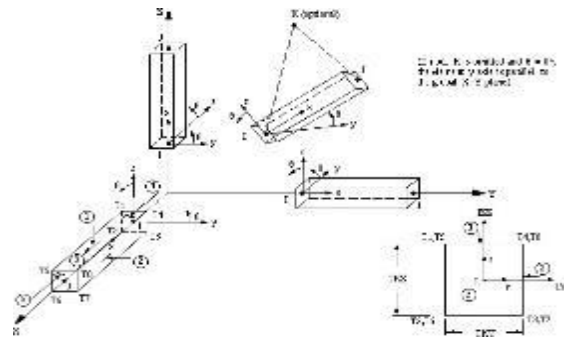


Figure 6: BEAM4 Element (ANSYS 18.1)

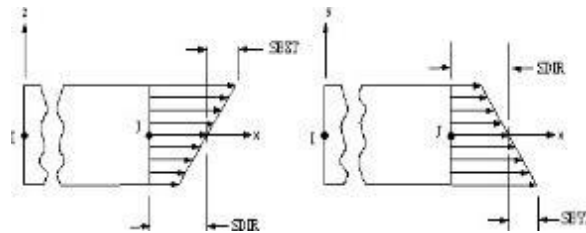


Figure 7: BEAM4 Element stress output (ANSYS 18.1)

Interface Element

CONTA174 is used to represent contact and sliding between 3-D target surfaces and a deformable surface defined by this element. The element is applicable to 3-D structural and coupled-field contact analyses. It can be used for both pair-based contact and general contact

CONTA174 is an 8-node element that is intended for general rigid-flexible and flexible-flexible contact analysis. In a general contact analysis, the area of contact between two (or more) bodies is generally not known in advance. CONTA174 is applicable to 3-D geometries. It may be applied for contact between solid bodies or shells.

In the case of pair-based contact, the target surface is defined by the 3-D target element type, TARGE170. In the case of general contact, the target surface can be defined by CONTA174 elements (for deformable surfaces) or TARGE170 elements (for rigid bodies only). It has the same geometric characteristics as the solid or shell element face with which it is connected as shown in **figure 8**.

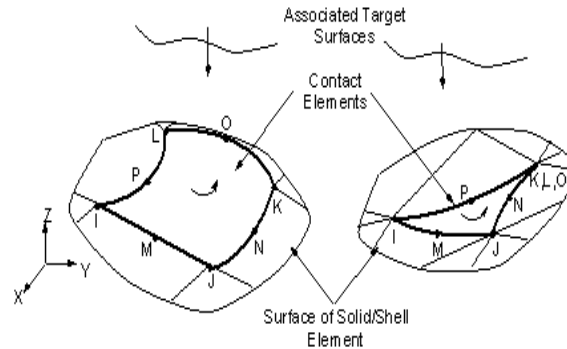


Figure 8: coordinate system for element type CONTA174 (ANSYS 18.1)

Real constant

SOLID 65

The element has one solid material and up to three rebar materials, which are input as real constants, include the material number MAT, volume ratio (VR), and the orientation angles (THETA, PHI).

The volume ratio is defined as the rebar volume divided by the total element volume. The orientation is defined by two angles (in degrees) from the element coordinate system.

BEAM4

The element is defined by two or three nodes, the cross-sectional area, two area moments of inertia (IZZ and IYY), two thickness (TKY and TKZ), an angle of orientation (Θ) about the element x-axis, the torsional moment of inertia(IXX), and the material properties, which are inputs as real constants for this element.

CONTA174

Contact wizard was used in this element to define the interface condition between the two surfaces of concrete, which was the behavior of contact surface, friction and initial adjustment, include the initial penetration and contact adjustment.

Materials

Concrete

Concrete was modeled as inelastic and multi-linear isotropic materials, which had a characteristic strength about 35 N/mm^2 for normal strength concrete and 60 N/mm^2 for high strength concrete. The stress-strain curve for each type of concrete was defined as shown in **figure 9 and 10**.

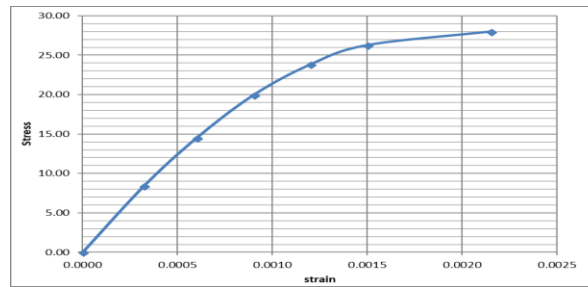


Figure 9: Stress- Strain curve for concrete of Fcu=35Mpa

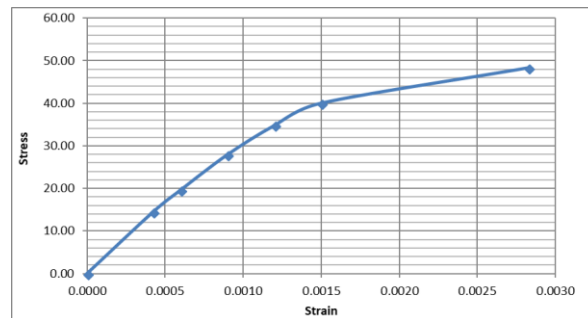


Figure 10: Stress- Strain curve for concrete of Fcu=60Mpa

Reinforcement rebars

Steel reinforcement was modeled as inelastic and bilinear isotropic material, which had yield strength of 400 N/mm^2 for main reinforcement and 240 N/mm^2 for secondary reinforcement and shear dowels.

Geometry and Dimensions

As the element type, real constant and material were defined, finite element analysis requires to meshing the specimen (divided into a number of small elements). In this study, specimen size was $(1060 \times 800 \times 100) \text{ mm}$, while the dimensions of the finite elements mesh were based on presence of steel reinforcement and shear dowels or not, the arrangement of steel reinforcement and its shape to divide the elements in between it.

In the monolithic specimen the finite element mesh was $47 \times 50 \times 25$, the three cases of loading which was uniform distributed load; one-line load and two-line load were shown in **figures 11 through 13**.

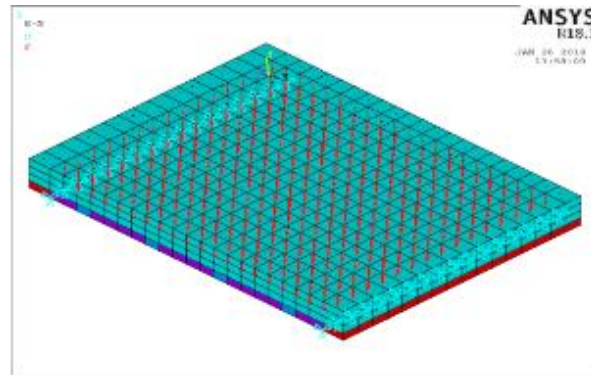


Figure 11: Modelling of uniformly distributed loads

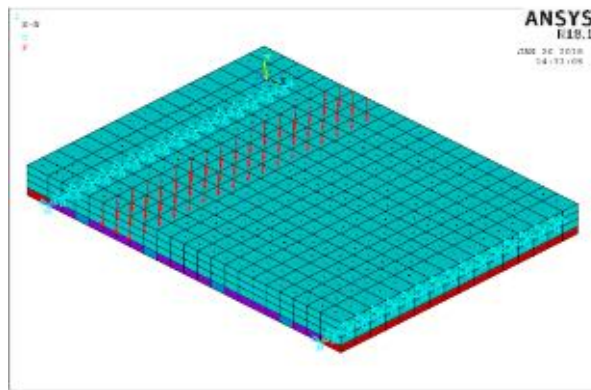


Figure 12: Modelling of one-line load

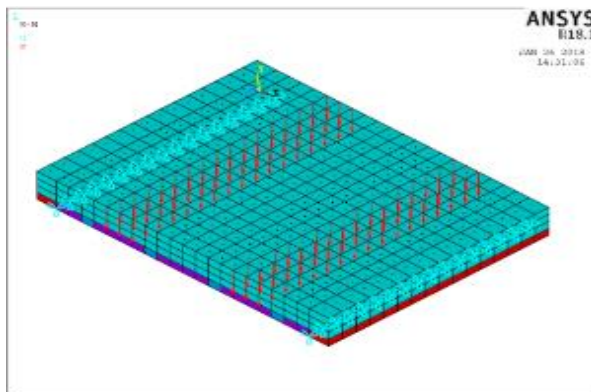


Figure 13: Modelling of two-line loads

Also, the different shear connector's distribution for the tested pre-slabs is shown in the **figures 14 through 17**.

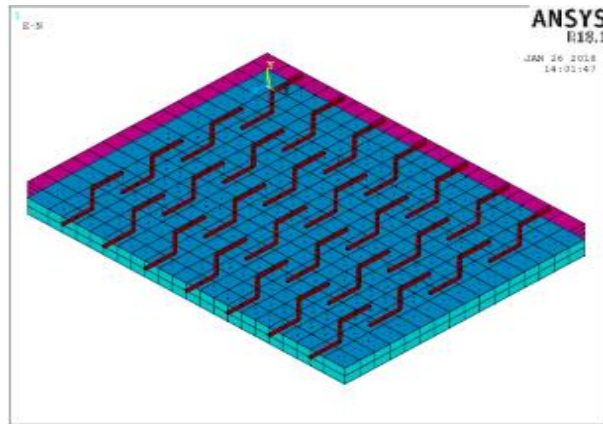


Figure 14: Modelling of pre-slab uniformly distributed dowels 0.1%

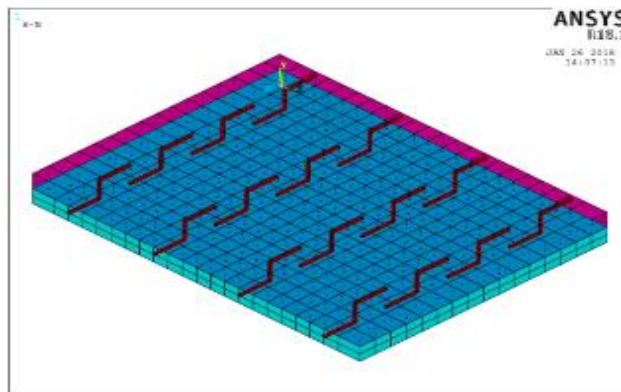


Figure 15: Modelling of pre-slab uniformly distributed dowels 0.06%

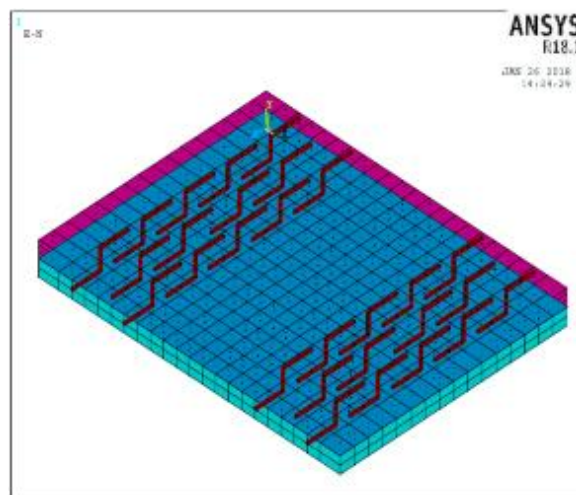


Figure 16: Modelling of pre-slab concentrated dowels 0.1%

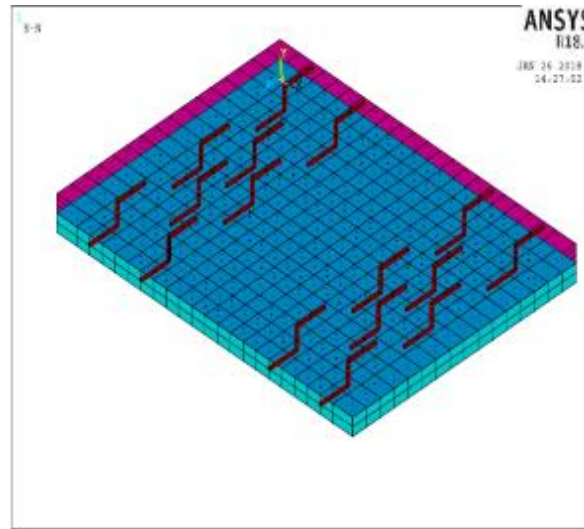


Figure 17: Modelling of pre-slab concentrated dowels 0.06%

Constrains

Simply supported with two lines of hinged supports were applied to all specimens as shown in **figure 13**.

Comparison between the theoretical and experimental results

Failure load

The theoretical and experimental failure load are plotted in **figure 18 through 20**, from which it can be observed that the theoretical failure load was about (86%: 98%) of that of the experimental failure load for pre-slabs (**R-N-U, 0.1%-U, 0.1%-O, 0.1%-O-R, 0.1%-T, 0.06%-U, 0.06%-O, 0.06%-O-R and 0.06%-T**), while for the other tested monolithic slabs and pre-slab the theoretical failure loads were approximately the same experimental failure loads.

From the previous results, it can be observed that the used modelling was sufficient enough to analyze both the monolithic slabs and pre-slabs where the experimental and the finite element model were in good agreement.

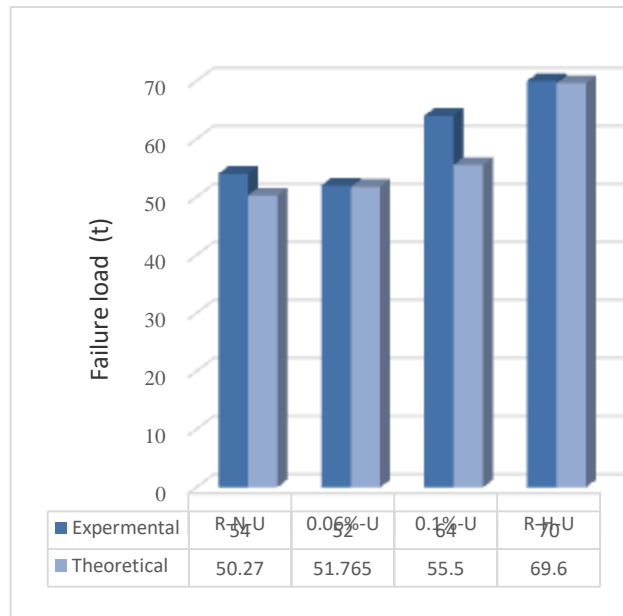


Figure 18: Failure load group 1

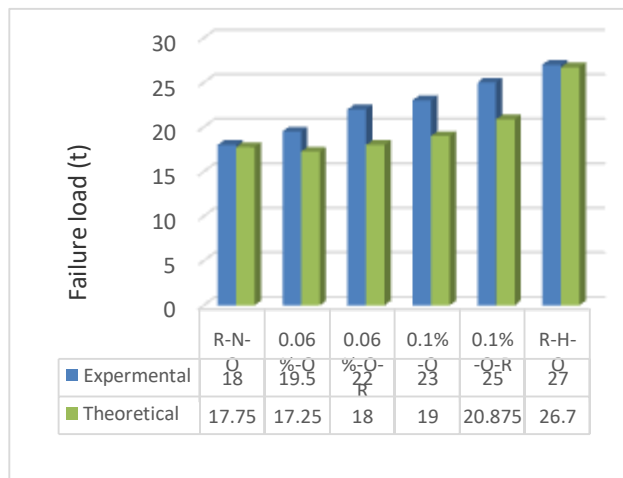


Figure 19: Failure load group 2&3

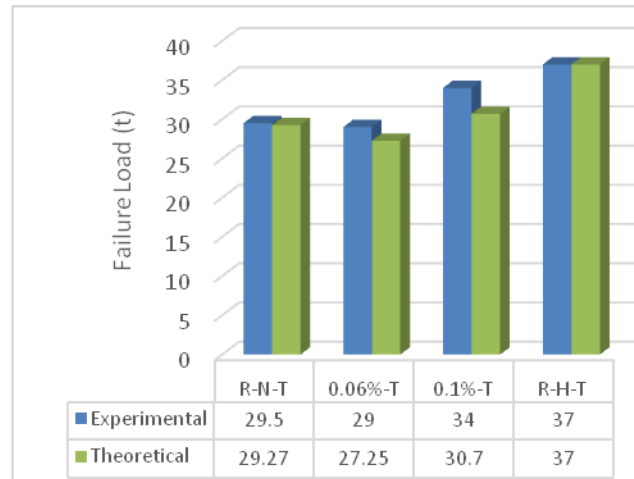


Figure 20: Failure load group 4

Ultimate shear strength

The ultimate shear strength at the interface of the tested specimens are calculated for both theoretical and experimental results and was showed in **figure 21, 22 and 23**.

From these three figures, it can be observed that the theoretical ultimate shear strength was about (76%: 95%) of that of the experimental results of the tested specimens unless for specimens (**R-H-U, R-N-O and R-H-T**) where the theoretical ultimate shear strength was approximately the same as the experimental ultimate shear strength. It can be found that the experimental and finite element model were in good agreement.

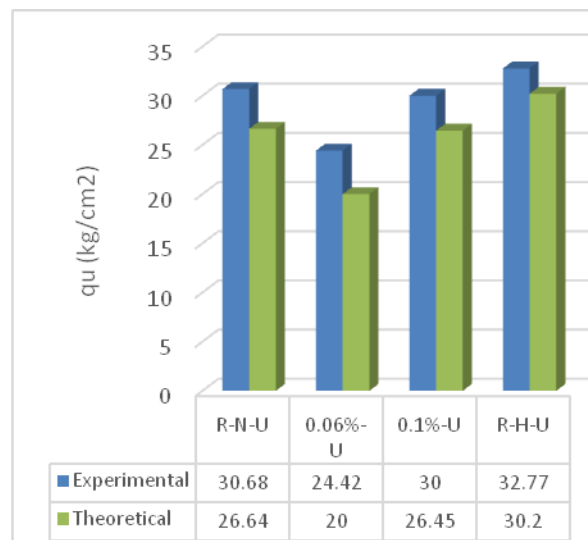


Figure 21: ultimate shear strength of tested slabs group 1

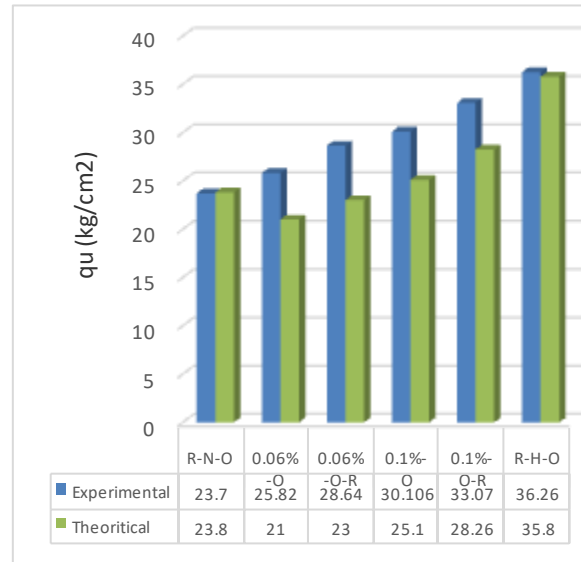


Figure 22: ultimate shear strength of tested slabs group 2&3

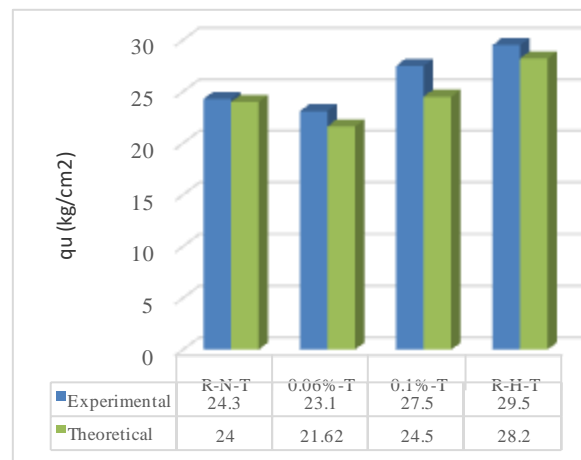


Figure 23: ultimate shear strength of tested slabs group 4

Load-Deflection

For **group1** the theoretical and experimental results of maximum deflections are plotted against the applied loads as shown in **figures 24**through **27**.

From **figure 24** of the monolithic specimen R-N-U, it can be observed that experimental and theoretical maximum deflection were approximately the same up to 30% of the experimental failure load and after that load level; the experimental maximum deflection appeared to be higher than the theoretical deflection. At the failure load level, the experimental maximum deflection was 38.5% higher over the theoretical maximum deflection.

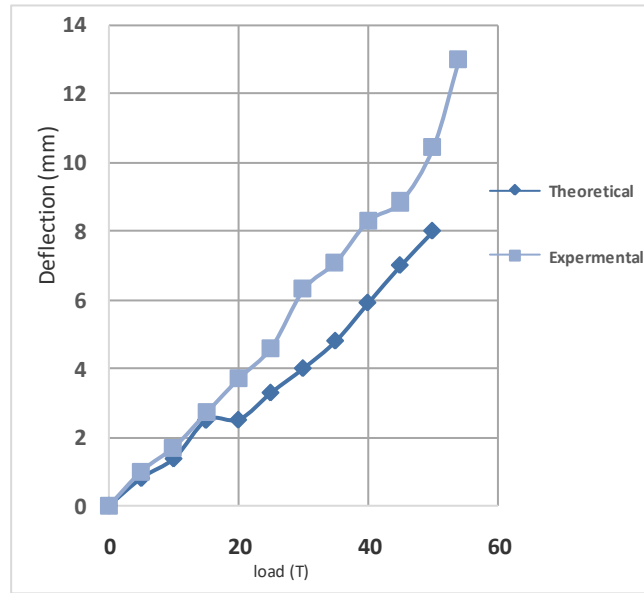


Figure 24: Load -deflection curve of slab R-N-U

From **figure 25** of the pre-slab 0.06%-U, it can be observed that experimental was higher than theoretical maximum deflection for all load levels with maximum variation of about 36%, at the ultimate load level.

From **figure 26** of the pre-slab 0.1%-U, it can be observed that experimental was higher than theoretical maximum deflection for all load levels with maximum variation especially at the beginning about 33%.

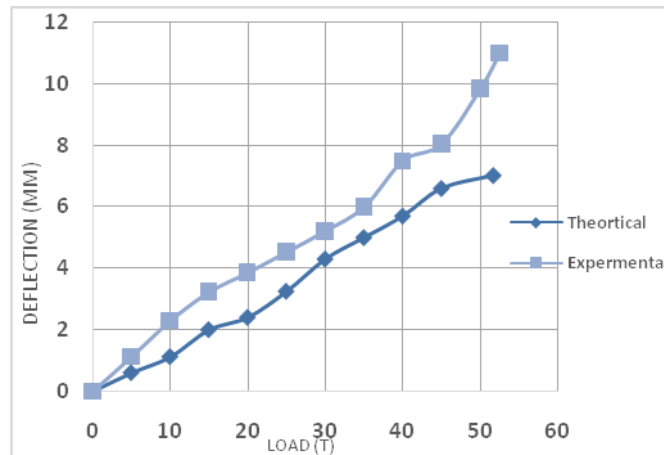


Figure 25: Load -deflection curve of slab 0.06%-U

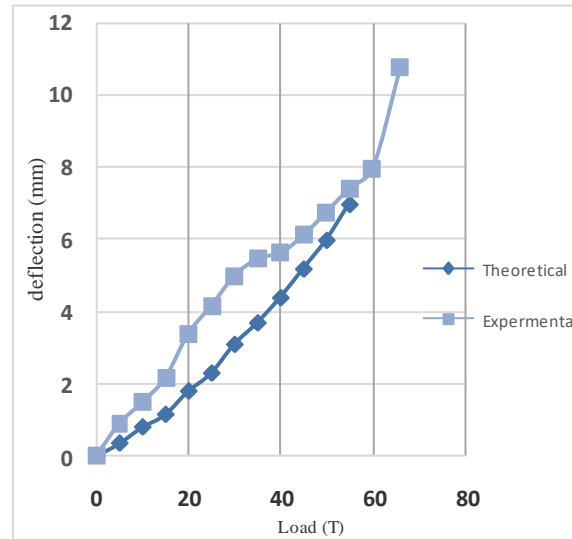


Figure 26: Load -deflection curve of slab 0.1%-U

From **figure 27** of the monolithic specimen R-H-U, it can be observed that both the experimental and theoretical maximum deflection were approximately the same.

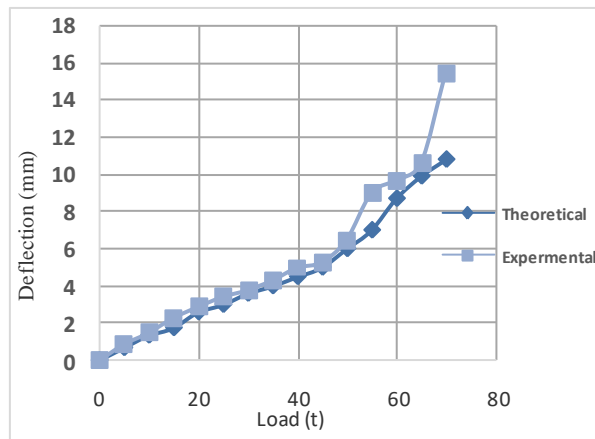


Figure 27: Load -deflection curve of slab R-H-U

For **group (2&3)** the theoretical and experimental results of maximum deflections are plotted against the applied loads as shown in **figures 28** through **33**.

From **figure 28** of the monolithic specimen R-N-O, it can be observed that experimental was higher than theoretical maximum deflection for all load levels with maximum variation of about 52% at the ultimate load level.

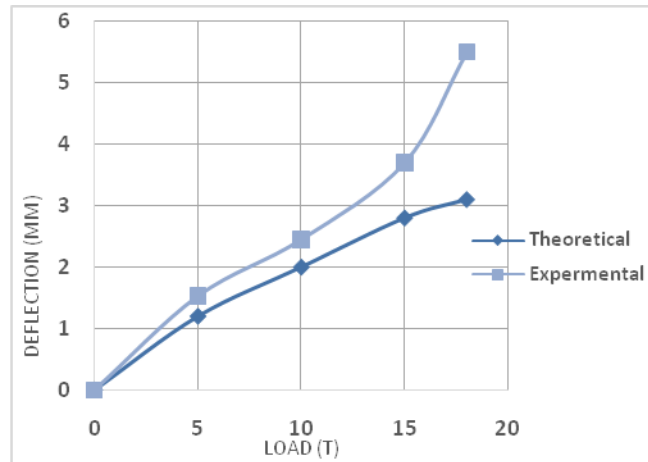


Figure 28: Load -deflection curve of slab R-N-O

From figures 29 ,30 and 31 of the pre-slabs (0.06%-O, 0.1%-O and 0.06%), it can be observed that experimental was higher than theoretical maximum deflection for all load levels with maximum variation of about (30% ,18% and 16%) respectively, at the ultimate load level.

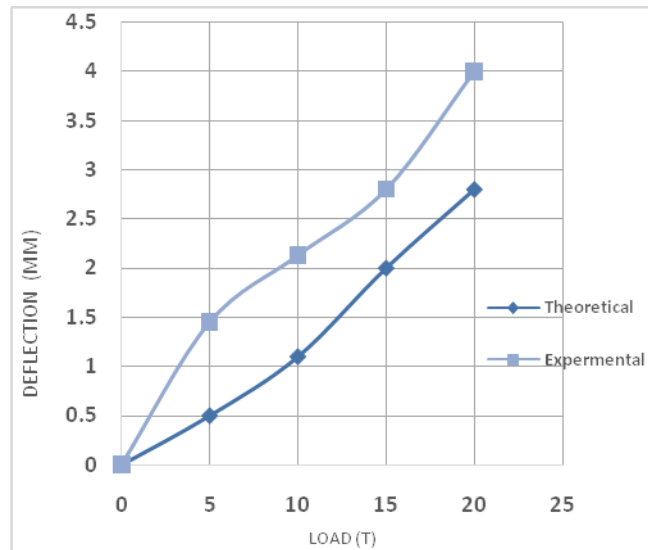


Figure 29: Load -deflection curve of slab 0.06%-O

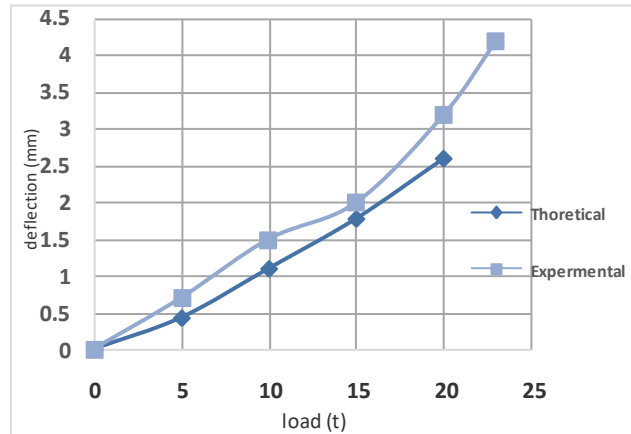


Figure 30: Load -deflection curve of slab 0.1%-O

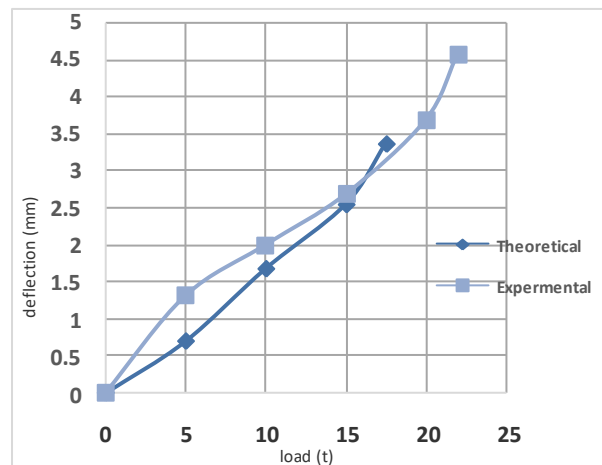


Figure 31: Load -deflection curve of slab 0.06%-O-R

From **figure 32** of the pre-slab 0.1-O-R, it can be observed that experimental and theoretical maximum deflection were approximately the same up to 25% of the experimental failure load and after that load level; the experimental maximum deflection appeared to be higher than the theoretical deflection. At the failure load level, the experimental maximum deflection was 31% higher over the theoretical maximum deflection.

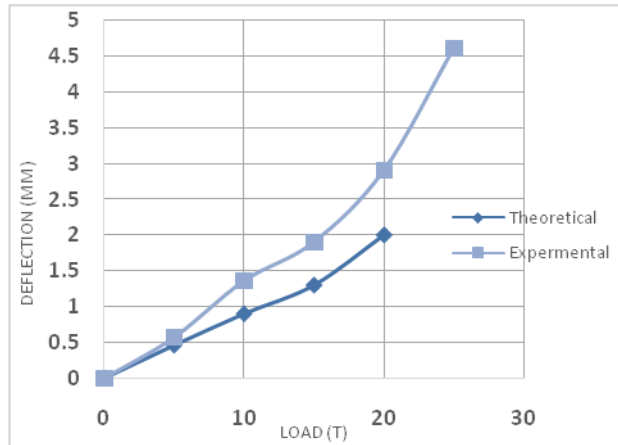


Figure 32: Load -deflection curve of slab 0.1%-O-R

From **figure 33** of the monolithic specimen R-H-O, it can be observed that both the experimental and theoretical maximum deflection were approximately the same up to 74% of the experimental failure load and after that load level, the experimental maximum deflection appeared to be higher than the theoretical deflection. At the failure load level, the experimental maximum deflection was 34% higher over the theoretical maximum deflection.

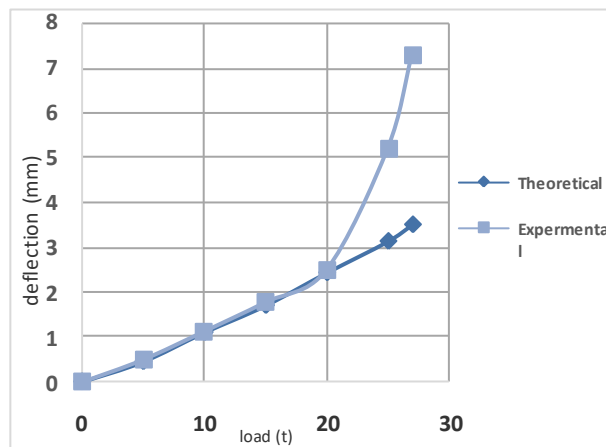


Figure 33: Load-deflection curve of slab R-H-O

For **group4** the theoretical and experimental results of maximum deflections are plotted against the applied loads as shown in **figures 34** through **37**.

From **figures 34** and **35** of specimens (R-N-T and 0.06%-T), it can be observed that experimental was higher than theoretical maximum deflection for all load levels with maximum variation of about (15.5% and 19%) respectively, at the ultimate load level.

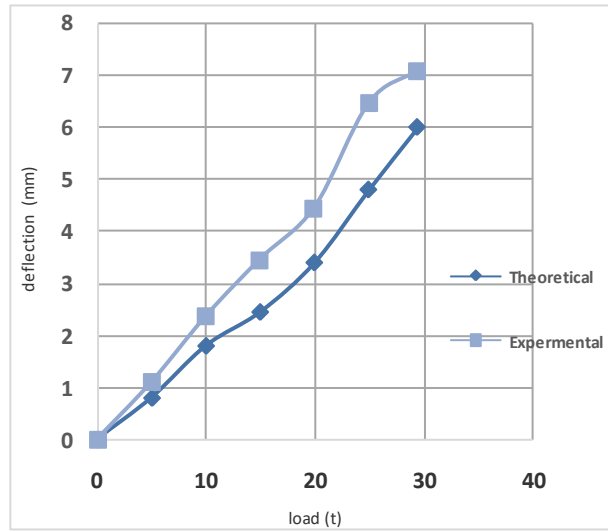


Figure 34: Load-deflection curve of slab R-N-T

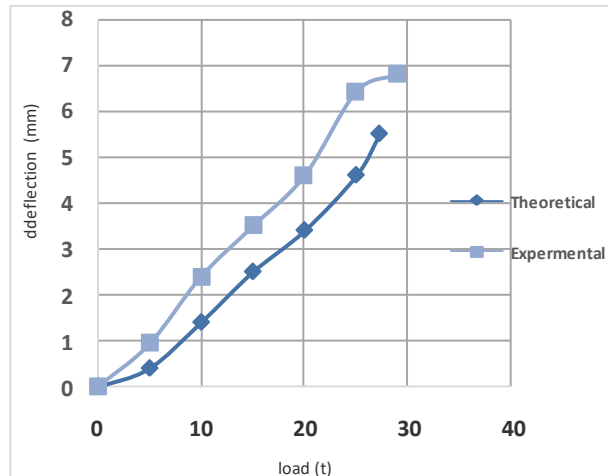


Figure 35: Load-deflection curve of slab 0.06%-T

From figures 36 and 37 of specimens (0.1%-T, R-H-T), it can be observed that both the experimental and theoretical maximum deflection were approximately the same up to 17% and 43% respectively, of the experimental failure load and after that load level, the experimental maximum deflection appeared to be higher than the theoretical deflection. At the failure load level, the experimental maximum deflection was 18% and 15.5% respectively, higher over the theoretical maximum deflection.

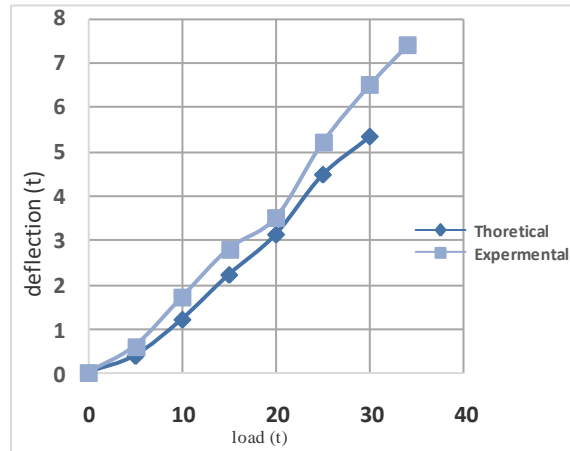


Figure 36: Load-deflection curve of slab 0.1%-T

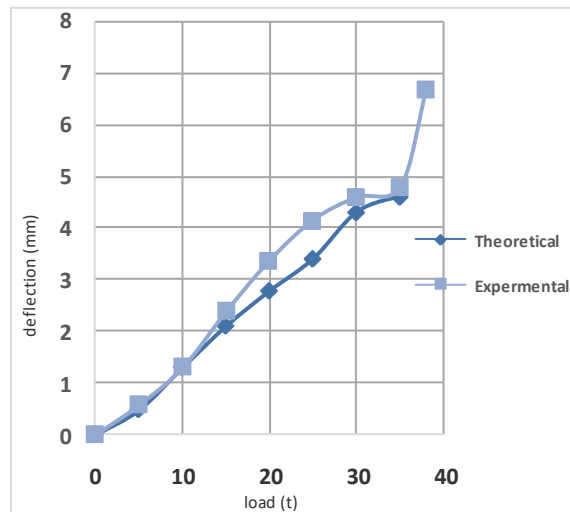


Figure 37: Load-deflection curve of slab R-H-T

Conclusion

- 1- The used finite element program (ANSYS 18.1) show close agreement with the experimental data of the full-scale RC tested specimens where;
 - (a) The theoretical failure loads were about (86%:100%) of that of experimental failure loads.
 - (b) The theoretical ultimate shear strength was about (76%:100%) loads of that of experimental results.
 - (c) Both the shear and flexure crack pattern had been approximately the same in both the theoretical analysis and experimental work.

- (d) Increase shear dowels ratio led to decrease in dowels' strain because of large dowels' cross-sectional area at the location of maximum shear stress along the interface area between two layers.
- (e) Load-deflection curve had been approximately the same in both the theoretical analysis and experimental program for refence and specimens with shear dowels 0.1%.

Reference

- 1-Ms.R.Sangeetha, Mr. P. S. Naufal Rizwan, Ms. S. Jansi Sheela, Mr. M. Franchis David, Mr.S. Daniel Raj," State of Art on Composite Slab Construction", International Journal of Applied Environmental Sciences ,Volume 13, Number 1 (2018), pp. 1-8.
- Kovach, J., & Naito, C., "Horizontal Shear Capacity of Composite Concrete Beams without Interface Ties" ATLSS REPORT NO. 08-05,Lehigh University 2008.
- Rabie, M., "Shear Transfer in Composite Reinforced Concrete Sections", Ph.D. Thesis. Faculty of Engineering. Cairo Univ., 1994.
- 4- Abd El-Hay A.S., "Shear transfer in composite continuous one-way pre-slabs", PH. D thesis. Faculty of Engineering, Cairo University 2006.